

2011

Robust high-temperature magnetic pinning induced by proximity in YBa₂Cu₃O₇₋₈/La_{0.67}Sr_{0.33}MnO₃ hybrids

C.Z Chen
Shanghai University China

Z Y. Liu
Shanghai University China

Y M. Lu
Shanghai University China

L Zeng
Shanghai University China

C B. Cai
Shanghai University China

See next page for additional authors

Follow this and additional works at: <https://ro.uow.edu.au/engpapers>

 Part of the [Engineering Commons](#)

<https://ro.uow.edu.au/engpapers/1360>

Recommended Citation

Chen, C.Z; Liu, Z Y.; Lu, Y M.; Zeng, L; Cai, C B.; Zeng, Rong; and Dou, S. X.: Robust high-temperature magnetic pinning induced by proximity in YBa₂Cu₃O₇₋₈/La_{0.67}Sr_{0.33}MnO₃ hybrids 2011.
<https://ro.uow.edu.au/engpapers/1360>

Authors

C.Z Chen, Z Y. Liu, Y M. Lu, L Zeng, C B. Cai, Rong Zeng, and S. X. Dou

Robust high-temperature magnetic pinning induced by proximity in $\text{YBa}_2\text{Cu}_3\text{O}_{7-\delta}/\text{La}_{0.67}\text{Sr}_{0.33}\text{MnO}_3$ hybrids

C. Z. Chen, Z. Y. Liu, Y. M. Lu, L. Zeng, C. B. Cai et al.

Citation: *J. Appl. Phys.* **109**, 073921 (2011); doi: 10.1063/1.3573491

View online: <http://dx.doi.org/10.1063/1.3573491>

View Table of Contents: <http://jap.aip.org/resource/1/JAPIAU/v109/i7>

Published by the American Institute of Physics.

Related Articles

Point-contact Andreev reflection spectroscopy of a magnetic superconductor $\text{Dy}_{0.6}\text{Y}_{0.4}\text{Rh}_{3.85}\text{Ru}_{0.15}\text{B}_4$
Low Temp. Phys. **38**, 1106 (2012)

Study of $\text{Bi}_2\text{Sr}_2\text{CaCu}_2\text{O}_8/\text{BiFeO}_3$ nano-composite for electrical transport applications
J. Appl. Phys. **112**, 053916 (2012)

Magnetoresistance in graphene-based ferromagnetic/ferromagnetic barrier/superconductor junction
J. Appl. Phys. **111**, 123908 (2012)

Electrical transport properties of (110)-oriented $\text{PrBa}_2(\text{Cu}_{0.8}\text{Ga}_{0.2})_3\text{O}_7$ thin films
Appl. Phys. Lett. **100**, 252601 (2012)

Two-dimensional magnetic field dependence of Josephson current and resonant current steps at finite voltage of square shape superconducting tunnel junctions
J. Appl. Phys. **111**, 113907 (2012)

Additional information on *J. Appl. Phys.*

Journal Homepage: <http://jap.aip.org/>

Journal Information: http://jap.aip.org/about/about_the_journal

Top downloads: http://jap.aip.org/features/most_downloaded

Information for Authors: <http://jap.aip.org/authors>

ADVERTISEMENT



AIP Advances

Now Indexed in Thomson Reuters Databases

Explore AIP's open access journal:

- Rapid publication
- Article-level metrics
- Post-publication rating and commenting

Robust high-temperature magnetic pinning induced by proximity in $\text{YBa}_2\text{Cu}_3\text{O}_{7-\delta}/\text{La}_{0.67}\text{Sr}_{0.33}\text{MnO}_3$ hybrids

C. Z. Chen,¹ Z. Y. Liu,^{1,a)} Y. M. Lu,¹ L. Zeng,¹ C. B. Cai,¹ R. Zeng,² and S. X. Dou²¹Research Center for Superconductors and Applied Technologies, Physics Department, Shanghai University, Shanghai 200444, China²Institute for Superconducting and Electronic Materials, University of Wollongong, NSW 2522, Australia

(Received 14 December 2010; accepted 1 March 2011; published online 15 April 2011)

An elaborately designed bilayer consisting of superconducting $\text{YBa}_2\text{Cu}_3\text{O}_{7-\delta}$ (YBCO) and ferromagnetic $\text{La}_{0.67}\text{Sr}_{0.33}\text{MnO}_{3-\delta}$ (LSMO) was prepared on a single crystal LaAlO_3 substrate by pulsed laser deposition (PLD), with a view to understanding the mechanism behind the influence of superconductor/ferromagnet proximity on the critical current density, J_c . The present bilayer system shows significant modifications in J_c , as evidenced by the suppressed decay of its temperature dependence, as well as the crossing behavior of the magnetic field dependence of J_c at high temperatures. This indicates that enhanced flux pinning emerges at high temperatures, and it is believed to arise from the special magnetic inhomogeneity, i.e., the ferromagnet/antiferromagnet clusters caused by phase separation due to the epitaxial stress between LSMO and the substrate. © 2011 American Institute of Physics. [doi:10.1063/1.3573491]

I. INTRODUCTION

Improvement of the critical current density, J_c , of high-temperature superconducting (HTSC) films is of great importance, not only for a fundamental understanding of vortex physics, but also for the application of coated conductors based on the epitaxial growth of $\text{YBa}_2\text{Cu}_3\text{O}_{7-\delta}$ (YBCO) films. It is well known that the critical current density of pure YBCO films can become very high due to a number of growth-induced structural defects such as dislocations.¹ For practical applications, however, the flux pinning in HTSC still needs to be further improved to overcome the giant vortex motion at high magnetic fields and high temperatures. Different attempts have been employed to enhance the flux-pinning performance of HTSC films, such as the engineering of substrates,² inclusion of precipitates,³ irradiation,⁴ rare-earth mixing,^{5,6} nanoparticle doping, quasimultilayers.^{7–9} Among these artificial techniques, one common feature is that they create high-density inhomogeneities with nanosized structures in the superconducting matrix. In the past several years, it has been frequently reported that strong c -axis correlated columnar defects, such as the self-assembled BaZrO_3 and BaSnO_3 nanodots achievable in YBCO films doped by homogeneous or heterogeneous additions, are very effective for the enhancement of flux pinning in high magnetic fields, especially as their directions are parallel to the c -axis, where the intrinsic pinning is absent.^{10–12} Recently Wee *et al.*¹³ reported similar columnar inclusions composed of $\text{Ba}_2\text{GdT}_2\text{O}_6$ (BGTO), leading to superior flux pinning, with the in-field J_c improved by a factor of 1.5–6 over the entire magnetic field range.

In reality, a number of efforts toward artificial manipulation of pinning centers in the past several years have only been limited to the pinning of vortex cores, with defect sizes

comparable to the superconducting coherence length ξ . The intrinsic disadvantage of the vortex core pinning is the rapid decrease in the pinning energy as the temperature increases, implying very small, even negligible, pinning potentials at applied temperatures close to T_c .¹⁴

To obtain considerable critical current density at high temperature, which is required for more electric-power applications, another type of flux pinning, called magnetic pinning, has been proposed.¹⁴ Magnetic pinning originates from the spatial modulation of the local magnetic field in superconductors on the length scale of the London penetration length, λ , which can be introduced into HTSC by various routes, such as regular arrays of ferromagnetic dots in the vicinity of superconducting films, or intrinsic magnetic domains in ferromagnet/superconductor (F/S) bilayers or multilayers, etc.¹⁵

The most distinctive characteristic of magnetic pinning is its robustness to the temperature. This is because such flux pinning acts on the whole vortex rather than on the vortex core alone.^{14,15} Moreover, magnetic pinning is more flexible under structural inhomogeneities compared with core pinning. The particular distribution of magnetization in ferromagnetic units can be changed by the magnetic field, which demonstrates a possible route to control superconducting currents via external magnetic fields. Vlasko-Vlasov *et al.*¹⁶ reported a rotatable, periodic, stripelike magnetic domain structure in F/S hybrids, in which the orientation of the magnetic domains can be arranged by the in-plane external magnetic field. Magneto-optical measurements revealed that the preferential flux lines enter along the direction of the domain walls. Thus, it is possible to guide vortex motion in a desirable direction and then manipulate its conductivity.

In our earlier work,¹⁷ we reported reduced broadening of the magnetoresistance (MR) in the vortex liquid region for an $\text{YBa}_2\text{Cu}_3\text{O}_{7-\delta}/\text{La}_{0.67}\text{Sr}_{0.33}\text{MnO}_{3-\delta}$ (YBCO/LSMO) bilayer, which was explained by magnetic pinning on the flux lines. The magnetic inhomogeneity in this system was

^{a)}Author to whom correspondence should be addressed. Electronic mail: zyliu@shu.edu.cn.

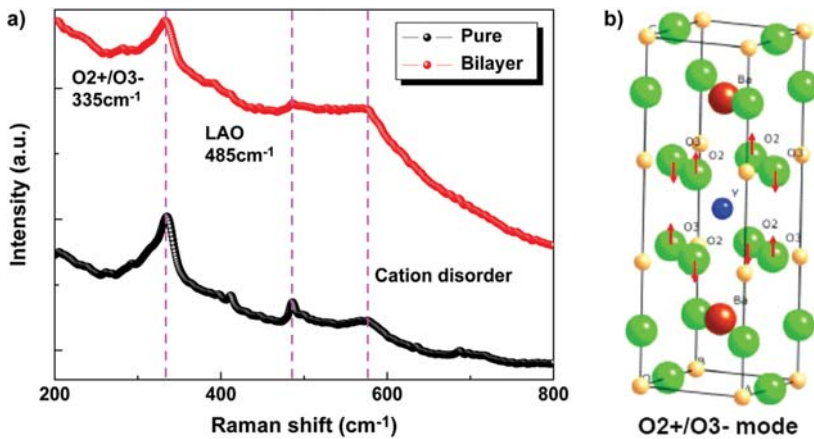


FIG. 1. (Color online) (a) Raman spectra of the YBCO/LSMO bilayer and the reference sample, a pure YBCO film. Three distinguishable modes with pronounced intensity are identified and categorized. (b) Configuration for the O2+/O3- phonon mode in YBCO lattices.

assumed to be caused by phase-separated clusters with ferromagnetic (FM) and antiferromagnetic (AFM) domains, which appear due to the epitaxial stress induced by the large mismatch between the LSMO and the substrate LaAlO₃ (LAO).

In the present paper, we have carried out a series of direct measurements of the critical current density and conducted a systematic investigation into the temperature dependence. We could then clarify the difference between the bilayer and a pure YBCO film. The present results disclose significant magnetic pinning effects arising from the ferromagnetic configurations, leading to a critical understanding of the mechanisms controlling the critical current density in ferromagnetic/superconducting (F/S) hybrids.

II. EXPERIMENTAL

The bilayer of YBCO (50 nm)/LSMO (40 nm), as well as the reference sample, a pure YBCO film 50 nm in thickness, were fabricated on single crystal (00 l) LAO substrates by pulsed laser deposition (PLD). Note that the thicknesses of the constituent layers of the studied bilayer were deliberately selected with the aim of achieving the best equilibrium between the magnetic pinning efficiency,¹⁸ subject to the YBCO thickness, and the superconductivity, subject to the LSMO thickness.¹⁹ More details related to sample preparation, such as deposition conditions, can be found in our previous publication.¹⁷

The crystal structure and epitaxial growth were examined by X-ray diffraction (XRD), which shows that all the studied samples exhibit perfect c -axis orientation and in-plane texture, with a full width at half maximum (FWHM) of less than 1.2°. The lattice relaxation was characterized by Raman spectroscopy, with the spectra collected in the back-scattering geometry, using a micro-Raman spectrometer (Renishaw in Via Plus) equipped with a charge-coupled device (CCD) detector. Transport and magnetization measurements were performed in a cryostat equipped with a 9 T magnet (Quantum Design PPMS-9T). Based on the transport measurements, the onset superconducting transition temperatures (90% ρ_n) are found to be 87.8 K and 88.6 K for the present bilayer and the pure film, respectively. The magnetization as a function of

temperature T and applied magnetic field H was recorded in the field region of $|H| \leq 5$ T and the temperature range of $5 \text{ K} \leq T \leq 80 \text{ K}$, from which the critical current density was extracted.

III. RESULTS AND DISCUSSION

Figure 1(a) shows the Raman spectra of the studied samples at room temperature. First, a sharp peak positioned at 485 cm⁻¹ is identified from the substrate.²⁰ With it, the precise positions of other Raman modes with appreciable intensity can be determined. Second, the mode occurring at 335 cm⁻¹ is identified, which is of most importance and interest, as it corresponds with the O2+/O3- mode,^{21,22} representing antisymmetric vibrations of O(2) and O(3) oxygen atoms in the YBCO lattice, as shown in Fig. 1(b). This mode is very sensitive to structural variation, and thus, a slight change in the crystal symmetry or lattice parameters may lead to an obvious frequency shift. In reality, it has been observed that there is a frequency shift of nearly 5 cm⁻¹ as the tetragonal phase of YBCO goes to the orthorhombic phase.²¹

Based on Raman spectroscopy, Chen *et al.*²³ reported that stress evolution and lattice distortion were induced by thickness variation and lattice misfit in LSMO films, which implies that there was structural modification of a LSMO film in a strained state. It is thus expected that the lattice vibrational frequencies of a stressed YBCO film should be different from those in its corresponding bulk material. In our case, however, no apparent shift within the experimental error ($\pm 1 \text{ cm}^{-1}$) is observed for the O2+/O3- mode. The bilayer and the pure YBCO film show the same Raman shift of 335 cm⁻¹, consistent with the values observed in YBCO bulks.²¹ This suggests that the 50 nm YBCO layer is completely relaxed, no matter what sublayer (here referring to LAO or LSMO) it grows on.

With the modified Bean critical state model,²⁴ the critical current densities for the studied films were evaluated by the widths of the magnetization loops, $\Delta M = |M^+| + |M^-|$, where $|M^+|$ and $|M^-|$ are descending and ascending branches, respectively. Figure 2 shows the field dependence of the critical current density for the bilayer at several given temperatures, which are characterized by a low-field plateau,

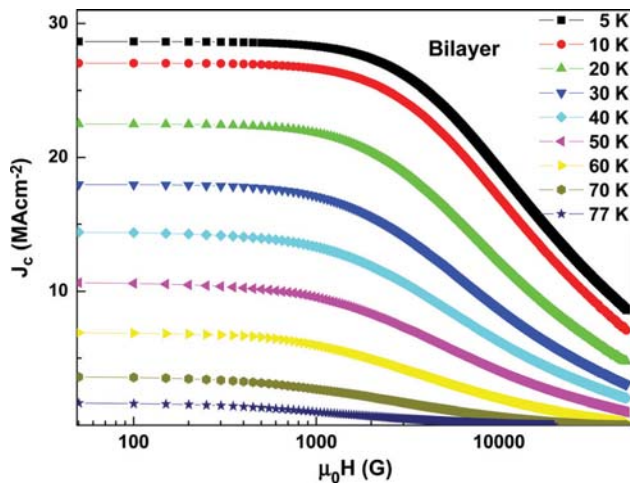


FIG. 2. (Color online) Field dependence of the critical current density for the bilayer at different temperatures. The J_c values are extracted from the magnetization curves.

followed by rapid decay in large magnetic fields. This is actually a common feature of all epitaxial high-temperature superconducting films.²⁵ In contrast to the pure YBCO film (not shown here), the present bilayer demonstrates two characteristics at least, i.e., reduced zero-field critical current density, $J_c(0)$, and an extended low-field plateau. Both characteristics have been observed as well in epitaxial YBCO films with artificial pinning centers.²⁶ However, the underlying physics may be different in this case. In the case of doped YBCO films, the decrease in $J_c(0)$ and the extension of the low-field plateau are believed to be caused by the reduced volume of the superconducting phase and the increased density of c -axis correlated defects, respectively. In the case of the present bilayer, however, the reduced superconducting volume and the increased correlated defects are hardly present. Instead, the potential mechanisms may arise from the suppressed superconductivity and the emergence of magnetic

pinning due to the proximity effect, as well as the residual field of the ferromagnetic layer.^{15,27}

Figure 3(a) shows the field dependence of the critical current density for the bilayer and the pure YBCO film at several given temperatures, which are characterized by the crossing (solid arrow) of two $J_c - H$ curves at high temperature. At low temperatures, such as 10 K, the pure YBCO shows a larger J_c over the whole magnetic field region. With increasing temperature, the difference in J_c between the two samples decreases, resulting in the obvious J_c crossover of the bilayer in the intermediate region of magnetic field. Similar crossover behavior of the $J_c - H$ curves has also been found in samples with artificial pinning as compared with undoped films.^{9,26,28,29}

Figure 3(b) shows our previous observations of such crossover behavior occurring in doped REBCO (RE = Y, Nd, etc.) films with different nanoparticle additions. The crossing results from the competition between the reduced J_c in zero magnetic field and the enhanced pinning in high magnetic field, with both of them caused by the structural disorder due to the doping. Further investigations show the temperature dependence of the crossing field, as marked by the dotted circles in Fig. 3(b). The higher the temperature, the larger the crossing field that is observed. In particular, at high temperatures such as 77 K, the crossing field shifts to very high magnetic field or disappears. This is unlike the crossover behavior found in the present bilayer, in which the crossing is even more apparent at elevated temperatures. In addition, another difference between the two systems is the observation of a second crossover point in the bilayer system, which can be clearly seen at high temperatures, such as 77 K (dashed arrow). Beyond this point and on, the bilayer shows the lower J_c again, indicating that a modification of the critical current density in the bilayer due to the proximity is prominent mainly at low and intermediate fields. And the J_c modification may originate from a different pinning mechanism, which shows robust pinning ability against the

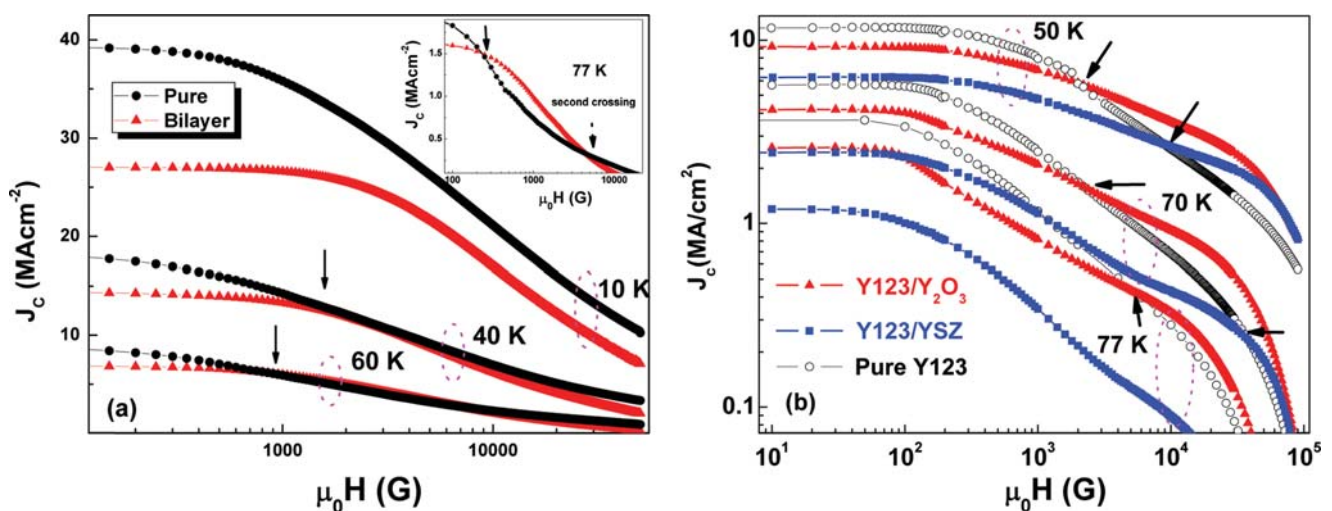


FIG. 3. (Color online) (a) Field dependence of the critical current density at three given temperatures of 10, 40, and 60 K for both the bilayer and the pure YBCO film. The inset gives the field dependence at 77 K, from which an obvious crossing is observed. (b) Field dependence of the critical current density at 50, 70, and 77 K for pure and doped YBCO films with different nanoparticle additions in a log-log plot. Arrows indicate the crossover of $J_c - H$ between them.

temperature. At high fields, however, the modification is weakened even disappears, which is thought to be related to the change in ferromagnetic configurations of the underlying LSMO by the external field and will be discussed in the last.

To further clarify the inherent mechanisms controlling or influencing the critical current density in the present bilayer, the temperature dependence of the critical current density, $J_c - T$, has been investigated. Note that the temperature dependence of the critical current density is commonly considered as an effective method to arrive at important implications regarding sample microstructures and flux pinning mechanisms. According to the theory of Blatter *et al.*,³⁰ vortices in type II superconductors can be pinned by a pinning site either through the spatial variations in the T_c throughout the material (“ δT_c pinning”) or by scattering of charge carriers with reduced mean free path near lattice defects (“ δl pinning”). In the framework of single vortex pinning, the temperature of the critical current density can be expressed by the form of $J_c(T) \propto [1 - (T/T_c)^2]^n$, with $n = 7/6$ in the case of δT_c pinning and $n = 5/2$ in the case of δl pinning.³¹ For practical epitaxial films with low-angle grain boundaries (GBs) or polycrystalline samples with complex networks of GBs, the $J_c(T)$ expression will be modified to a more simplified form, $J_c = J_0(1 - T/T_c)^n$, where the n value depends on the type of contact between GBs, such as $n = 1$ for the contact in superconductor-insulator-superconductor (SIS) structures, $n = 2$ for the contact in superconductor-normal metal-superconductor (SNS) structures, and $n = 3/2$ for the contact in SNIS structures.^{32,33} Note that the power law is based on the Ginzburg-Landau theory, where the two characteristic lengths λ and ξ show the same temperature dependence of $\lambda, \xi \propto (1 - T/T_c)^{-1/2}$ in the case of T close to T_c .

Figure 4 shows the temperature dependence of the zero-field critical current density for the present bilayer and the pure film. The data were obtained in a remanent state with very low flux densities, allowing the temperature dependence to be discussed within the framework of individual flux line pinning. The formula $J_c = J_0(1 - T/T_c)^n$ with two parameters J_0 and n is used to fit the above $J_c - T$ curves. The exponent of $n = 1.48$ for the pure sample is very close to $3/2$, which was observed by Fedotov *et al.*³⁴ in epitaxial YBCO films. This seems to support contacts of the SNIS type.

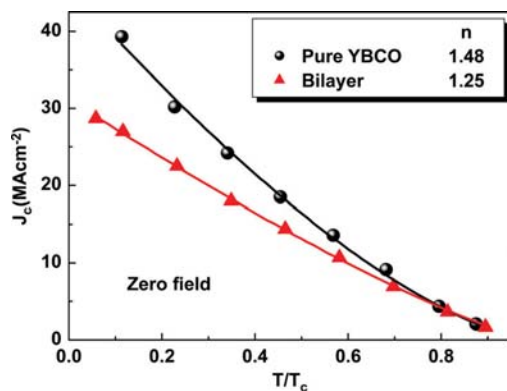


FIG. 4. (Color online) Temperature dependences of the zero-field critical current density for the bilayer and the pure YBCO film. Solid lines are a fit to $J_c = J_0(1 - T/T_c)^n$.

However, this conjecture is not in agreement with the high current density in those epitaxial films. Here, we recollect the case of strong vortex core pinning with narrow correlated defects, which predicts the exponent of $n = 3/2$, as being more applicable to our case.³⁵

On the other hand, the exponent of $n = 1.25$ is found for the bilayer, which is significantly smaller than $n = 1.48$ for the pure YBCO film. The difference in the n value between the bilayer and the pure film seems subtle but not trivial. The bilayer shows a suppressed decay of the critical current with increasing temperature as the exponent n decreases. Again, this demonstrates its robust pinning performance against the temperature.

It is interesting to note that the exponent n is dependent on the applied magnetic field, as the empirical formula $J_c = J_0(1 - T/T_c)^n$ is applied to describe the $J_c(T)$ relation in magnetic field. As shown in Fig. 5, the exponent n of the pure film increases quickly as the magnetic field increases, and then saturates in a field of about 1 T. This is very different from the case of the bilayer, where the n increases monotonically up to the maximum field of 5 T. The difference in $n-H$ relations implies different mechanisms, which may originate from the influence of the ferromagnet on the properties of the critical current. Obviously, the magnetization configuration in the ferromagnetic layer is subject to the external field, implying that magnetic pinning and associated J_c modification are sensitive to applied magnetic fields.

As mentioned before, the enhanced flux pinning at high temperatures for the present bilayer is believed to arise from the magnetic pinning, where the magnetic inhomogeneity may be caused by the phase-separated FM/AFM clusters that exist due to the epitaxial stress between LSMO and the substrate. It is also possible that the phase separation takes place on the submicrometer scale along with the coexistence of giant clusters, since there is already evidence for such macroscopic phase separation in manganite films, both experimentally and theoretically.^{36–38} Due to the comparable length scales between the London penetration length λ and

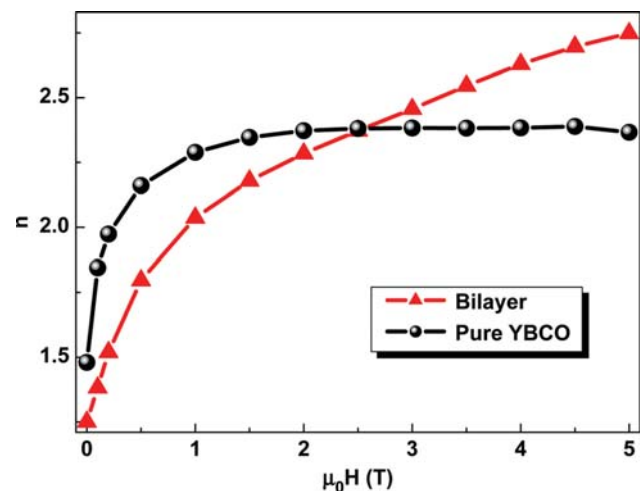


FIG. 5. (Color online) Field dependence of the fitting exponent n for the present bilayer and the pure sample. The n values are obtained from the fitting to $J_c = J_0(1 - T/T_c)^n$ at different magnetic fields.

the size of phase-separated clusters, spatial modulation of the local field in the superconductor will result in effective magnetic pinning in the bilayer.

On the other hand, the patterns of magnetic inhomogeneity will be altered by the external field, owing to the increase in FM domains, accompanied by the melting of insulating AFM clusters.³⁹ This leads to weakened magnetic inhomogeneity, and thus the efficiency of magnetic pinning decreases. Eventually, the corresponding modification in the properties of the critical current by the magnetic field is manifested in the form of the observed monotonic n - H dependence as well as the presence of the second crossover point in the bilayer system.

IV. CONCLUSIONS

In summary, the structural characteristics and the properties of the critical current density for a YBCO/LSMO bilayer have been studied with respect to the flux pinning mechanism, which is understood to be due to superconductor/ferromagnet proximity. Compared to the pure YBCO films, the present bilayer shows robust pinning performance against temperature, as evidenced by the direct observation of slower decay of the temperature dependence of J_c , as well as the obvious crossing of the $J_c - H$ curves at high temperatures. The enhanced flux pinning at high temperatures is believed to arise from magnetic pinning, since magnetic inhomogeneity exists due to phase-separated FM/AFM clusters induced by the epitaxial stress between the LSMO and the substrate.

ACKNOWLEDGMENTS

This work is partly sponsored by the Ministry of Science and Technology of China (973 Projects, No. 2011CBA00105, and 863 Projects, No. 2009AA03Z204), the Science and Technology Commission of Shanghai Municipality (No. 10dz1203500), the Innovation Fund for PhD Graduates of Shanghai University (No. SHUCX101063) and Australian Research Council Discovery Grant (DP0770205). The supports from the Open Project of State Key Laboratory of Functional Materials for Informatics (Chinese Academy of Sciences), and the Shanghai Leading Academic Discipline Project (No. S30105) are gratefully acknowledged as well.

¹B. Dam, J. M. Huijbregtse, F. C. Klaassen, R. C. F. van der Geest, G. Doornbos, J. H. Rector, A. M. Testa, S. Freisem, J. C. Martinez, B. Stäuble-Pümpin, and R. Griessen, *Nature* **399**, 439 (1999).

²A. Crisan, S. Fujiwara, J. C. Nie, A. Sundaresan, and H. Ihara, *Appl. Phys. Lett.* **79**, 4527 (2001).

³A. N. Grigorenko, S. J. Bending, G. D. Howells, and R. G. Humphreys, *Phys. Rev. B* **62**, 721 (2000).

⁴T. Schuster, H. Kuhn, M. R. Koblishka, H. Theuss, H. Kronmüller, M. Leghissa, M. Kraus, and G. Saemann-Ischenko, *Phys. Rev. B* **47**, 373 (1993).

⁵C. Cai, B. Holzapfel, J. Hänisch, L. Fernández, and L. Schultz, *Appl. Phys. Lett.* **84**, 377 (2004).

⁶J. L. MacManus-Driscoll, S. R. Foltyn, Q. X. Jia, H. Wang, A. Serquis, B. Maiorov, L. Civale, Y. Lin, M. E. Hawley, M. P. Maley, and D. E. Peterson *Appl. Phys. Lett.* **84**, 5329 (2004).

⁷T. Haugan, P. N. Barnes, R. Wheeler, F. Meisenkothen, and M. Sumpston, *Nature* **430**, 867 (2004).

⁸J. Hänisch, C. Cai, R. Hühne, L. Schultz, and B. Holzapfel, *Appl. Phys. Lett.* **86**, 122508 (2005).

⁹C. Cai, J. Hänisch, R. Hühne, V. Stehr, C. Mickel, T. Gemming, and B. Holzapfel, *J. Appl. Phys.* **98**, 123906 (2005).

¹⁰A. Goyal, S. Kang, K. J. Leonard, P. M. Martin, A. A. Gapud, M. Varela, M. Paranthaman, A. O. Ijaduola, E. D. Specht, J. R. Thompson, D. K. Christen, S. J. Pennycook, and F. A. List, *Supercond. Sci. Technol.* **18**, 1533 (2005).

¹¹S. Kang, A. Goyal, J. Li, A. A. Gapud, P. M. Martin, L. Heatherly, J. R. Thompson, D. K. Christen, F. A. List, M. Paranthaman, and D. F. Lee, *Science* **311**, 1911 (2006).

¹²C. V. Varanasi, P. N. Barnes, J. Burke, L. Burke, I. Maartense, T. J. Haugan, E. A. Stinzianni, K. A. Dunn, and P. Haldar, *Supercond. Sci. Technol.* **19**, L37 (2006).

¹³S. H. Wee, A. Goyal, E. D. Specht, C. Cantoni, Y. L. Zuev, and S. Cook, *Phys. Rev. B* **81**, 140503(R) (2010).

¹⁴L. N. Bulaevskii, E. M. Chudnovsky, and M.P. Maley, *Appl. Phys. Lett.* **76**, 2594 (2000).

¹⁵A. Y. Aladyshev, A. Y. Silhanek, W. Gillijns, and V. V. Moshchalkov, *Supercond. Sci. Technol.* **22**, 053001 (2009).

¹⁶V. Vlasko-Vlasov, U. Welp, G. Karapetrov, V. Novosad, D. Rosenmann, M. Iavarone, A. Belkin, and W.-K. Kwok, *Phys. Rev. B* **77**, 134518 (2008).

¹⁷C. Z. Chen, C. B. Cai, L. Peng, B. Gao, F. Fan, Z. Y. Liu, Y. M. Lu, R. Zeng, and S. X. Dou, *J. Appl. Phys.* **106**, 093902 (2009).

¹⁸H.-U. Habermeier, J. Albrecht, and S. Soltan, *Supercond. Sci. Technol.* **17**, S140 (2004).

¹⁹Z. Sefrioui, M. Varela, V. Peña, D. Arias, C. León, J. Santamaría, J. E. Villegas, J. L. Martínez, W. Saldarriaga, and P. Prieto, *Appl. Phys. Lett.* **81**, 4568 (2002).

²⁰Y. M. Xiong, T. Chen, G. Y. Wang, X. H. Chen, X. Chen, and C. L. Chen, *Phys. Rev. B* **70**, 094407 (2004).

²¹K. Venkataraman, R. Baurceau, and V. A. Maroni, *Appl. Spectrosc.* **59**, 639 (2005).

²²V. A. Maroni, Y. Li, D. M. Feldmann, and Q. X. Jia, *J. Appl. Phys.* **102**, 113909 (2007).

²³C. Z. Chen, C. B. Cai, Z. Y. Liu, L. Peng, B. Gao, F. Fan, Y. M. Lu, R. Zeng, Z. P. Guo, W. X. Li, and S. X. Dou, *Solid State Commun.* **150**, 66 (2010).

²⁴A. M. Campbell and J. E. Evetts, *Adv. Phys.* **21**, 199 (1972).

²⁵C. Cai, B. Holzapfel, J. Hänisch, L. Fernández, and L. Schultz, *Phys. Rev. B* **69**, 104531 (2004).

²⁶S. R. Foltyn, L. Civale, J. L. MacManus-Driscoll, Q. X. Jia, B. Maiorov, H. Wang, and M. Maley, *Nat. Mater.* **6**, 631 (2007).

²⁷A. I. Buzdin, *Rev. Mod. Phys.* **77**, 935 (2005).

²⁸C. Cai, B. Holzapfel, J. Hänisch, and L. Schultz, *Phys. Rev. B* **70**, 064504 (2004).

²⁹L. Peng, C. Cai, C. Chen, Z. Liu, J. Liu, B. Gao, and J. Zhang, *J. Phys. D: Appl. Phys.* **41**, 155403 (2008).

³⁰G. Blatter, M. V. Feigel'man, V. B. Geshkenbein, A. I. Larkin, and V. M. Vinokur, *Rev. Mod. Phys.* **66**, 1125 (1994).

³¹R. Griessen, H. H. Wen, A. J. J. van Dalen, B. Dam, J. Rector, and H. G. Schnack, *Phys. Rev. Lett.* **72**, 1910 (1994).

³²D. G. Steel, J. D. Hettinger, F. D. Yuan, J. Miller, K. E. Gray, J. H. Kang, and J. Talvacchio, *Appl. Phys. Lett.* **68**, 120 (1996).

³³E. A. Pashitskii, V. I. Vakaryuk, S. M. Ryabchenko, and Y. V. Fedotov, *J. Low Temp. Phys.* **105**, 1261 (2001).

³⁴Y. V. Fedotov, S. M. Ryabchenko, and A. P. Shakhov, *Fiz. Nizk. Temp.* **26**, 638 (2000).

³⁵V. Pan, Y. Cherpak, V. Komashko, S. Pozigun, C. Tretiachenko, A. Semenov, E. Pashitskii, and A. V. Pan, *Phys. Rev. B* **73**, 054508 (2006).

³⁶M. Fäth, S. Freisem, A. A. Menovsky, Y. Tomioka, J. Aarts, and J. A. Mydosh, *Science* **285**, 1540 (1999).

³⁷A. Moreo, M. Mayr, A. Feiguin, S. Yunoki, and E. Dagotto, *Phys. Rev. Lett.* **84**, 5568 (2000).

³⁸L. Zhang, C. Israel, A. Biswas, R. L. Greene, and A. de Lozanne, *Science* **298**, 805 (2002).

³⁹E. Dagotto, *New J. Phys.* **7**, 67 (2005).